

# SPIRAL 2 resonators

G. Devanz DSM/DAPNIA, CEA/Saclay, F91191 Gif-sur-Yvette

## Abstract

The SPIRAL 2 project to be built in GANIL is a high intensity ion linear accelerator for radioactive beam production. Most of the acceleration is provided by twenty four 88 MHz quarter wave resonators breaking into two beta families. The first ( $\beta=0.07$ ) was developed at CEA-Saclay, while the second ( $\beta=0.12$ ) was studied at IPN-Orsay. Each team has carried out the integration study of the QWRs in their respective cryomodule taking into account tight longitudinal space requirements. Prototypes of each cavity type have been built, prepared and tested in vertical cryostats. We present the RF and mechanical design of the resonators, cryostats, the preparation and test equipment specifically developed for QWRs, as well as the RF test results.

## 1 INTRODUCTION

The superconducting linac of SPIRAL 2 [1] accelerates a 5 mA deuteron beam from 1.5 MeV at the RFQ exit up to 40 MeV, thus covering a large span of reduced velocity, from 0.04 to 0.2. Independently phased quarter-wave (QWR) or half-wave (HWR) resonators are the cavities of choice for this purpose, and have been adopted in a large number of existing or proposed machines [2, 3, 4]. The operation temperature is 4.5 K, the RF frequency 88.05 MHz and the cavities are in bulk niobium. The linac design lead to the definition of two  $\beta$  families of quarter wave cavities [5]. The first SRF linac section is made of 12  $\beta=0.07$  QWRs and the high energy section comprises 12  $\beta=0.12$  QWRs. The transition  $\beta$  is 0.11. Room temperature quadrupoles have been chosen for transverse focusing since higher alignment tolerances can be achieved compared to superconducting solenoids. On the bad side, they require a shorter lattice which puts stringent conditions on the cryostats longitudinal dimensions. Another consequence is the need for short cryostats: while lower  $\beta$  cavities are hosted in an individual cryostat, high  $\beta$  cavities are grouped in pairs in a single cryostat.

## 2 RESONATOR DESIGN

In various laboratories, a large number of elliptic SC cavities have reached routinely peak electric surface field ( $E_{pk}$ ) exceeding 40 MV/m without field emission provided they were prepared and high pressure rinsed in a clean room. Another requirement for high field reliable operation in the linac is that the cavity vacuum is kept separated from the cryostat insulation vacuum. This rating of 40 MV/m has been chosen as the design limit on the peak field for the QWRs in SPIRAL 2. The peak magnetic field ( $B_{pk}$ ) upper limit is fixed at 80 mT. Although the maximum operating

gradient is 6.5 MV/m, the design gradient is 8 MV/m which sets the upper limit for the  $E_{pk}/E_{acc}$  ratio at 5 and the maximum value for the  $B_{pk}/E_{acc}$  ratio at 10 mT/(MV/m). In this paper, we use the definition  $E_{acc} = V_{acc}/(\beta_{opt}\lambda)$ , where  $V_{acc} = |\int E_z(z)e^{i\omega z/\beta c} dz|$  in order to have a shape independent definition for the accelerating field. The  $\beta=0.07$  QWRs RF design was carried out using Ansoft HFSS v8.5 and Vector Fields SOPRANO v8.7 whereas the  $\beta=0.12$  QWRs where designed with CST Mafia 4.1 (fig. 1).

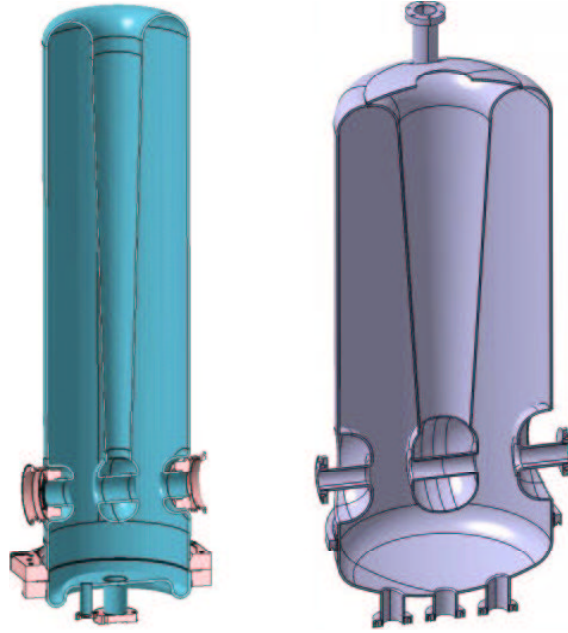


Figure 1:  $\beta=0.07$  (left) and  $\beta=0.12$  (right) QWRs

The main RF parameters of the cavity are displayed in table 1.

frequency [MHz]	88.05	88.05
$\beta_{opt}$	0.07	0.12
$E_{pk}/E_{acc}$	5.0	5.6
$B_{pk}/E_{acc} [\frac{mT}{MV/m}]$	8.9	10.2
r/Q [ $\Omega$ ]	632	518
$V_{acc}$ at 6.5 MV/m, $\beta_{opt}$ [MV]	1.54	2.65
G [ $\Omega$ ]	22.4	38
beam tube $\phi$ [mm]	30	36
cavity ext. $\phi$ [mm]	230	380
$Q_{ext}$	$6.6 \cdot 10^5$	$1.1 \cdot 10^6$

Table 1: characteristics of  $\lambda/4$  cavities

The  $E_{pk}/E_{acc}$  ratio was reduced by optimization of the drift tubes dimensions and  $B_{pk}/E_{acc}$  by a careful choice of the stem conical part radii. All the cavities in the linac will be powered by the same coaxial power coupler designed

by LPSC-Grenoble [6]. The nominal power carried by the coupler is 15 kW CW. The coupler port is located on the bottom plate of the resonators, in the low magnetic field region to avoid losses on the normal conducting coupler tip.

### 3 $\beta=0.07$ RESONATORS

#### 3.1 Mechanical design

The cavity is made from Nb sheet to reach a 4 mm thickness after chemical etching, except the stem, welding and brazing areas which are thinner. The lower  $\beta$  resonator has a dismountable bottom plate in order to provide a large aperture for the high pressure rinsing system and ease the flow. A special copper gasket and stainless steel CF flanges ensure both vacuum tightness and RF contact between the bottom plate and the cavity. The stainless steel He tank is welded on this flange so it does not enclose the bottom plate. This makes its design simpler, since neither the power coupler, field probe or pumping tube need to go through it. The dismountable plate is made of Nb deposited copper. It has a special profile in order to keep the flange at a low position to minimize the losses in the RF gasket. The 'S' shape provides the mechanical compliance needed to protect the stainless steel to copper brazing during cooldown. It is also compatible with the pressure qualification tests required for vertical cryostat testing. The heat flux on the bottom plate brought by the power coupler is expected to be about 1 W. Thanks to its high thermal conductivity, the Nb/Cu plate can be cooled only by means of a set of braids connected to the He tubing (fig. 2).

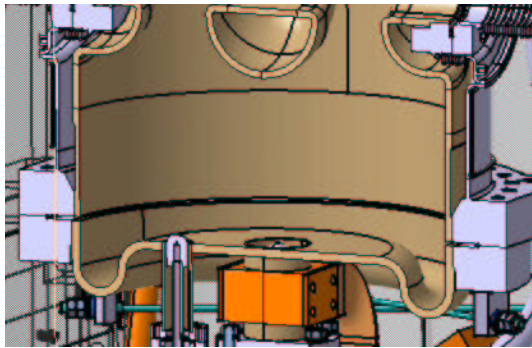


Figure 2: Bottom plate

The gasket is a modified CF copper gasket which ensures RF contact. The induced losses at nominal field are 26 mW, to be compared to the expected 1.75 W in the superconducting parts of the cavity, assuming a surface resistance of 10 n $\Omega$ .

#### 3.2 Cold tuning system

Beam dynamics set stringent requirements on the overall length of the low  $\beta$  cryomodule which prevents the installation of a cold tuning system (CTS) that would act di-

rectly on the beam tubes and change the gaps length. To overcome this problem, the cavity can be tuned by squeezing the outer cylinder perpendicular to the beam axis. The circular cross section is locally changed into an elliptical shape, which in turn acts on the gap length. The position and the shape of the CTS feet that are welded to the cavity have been optimized in order to maximize the tuning range at 4K. During tuning, stress in the cavity material must not exceed the yield stress  $\sigma_y$  otherwise plastic deformation would occur. For niobium, the yield stress changes dramatically between 300 K ( $\sigma_y \simeq 50$  MPa) and 4 K ( $\sigma_y \simeq 400$  MPa), the tuning range will thus be much wider in cryogenic operation than at room temperature. Full 3D coupled mechanical-RF computations have been carried out, using CEA CASTEM FEM code for the mechanical part, and SOPRANO on a unique mesh generated in I-DEAS. The output of both mechanical and RF codes are fed to a routine based on Slater perturbation method, which computes the detuning resulting from cavity deformation and surface fields. For the optimal position of the CTS feet which is about 100 mm above the beam axis, the tuning range at 4 K is  $\pm 25$  kHz. The mechanical system itself is an evolution of the well proven level arm type design used for TTF, SOLEIL and Super-3HC[7]. The motor can be installed either on the cold mass or outside the cryostat. In the later case an articulated shaft transmits the motor rotation to the gear box (figure 3).

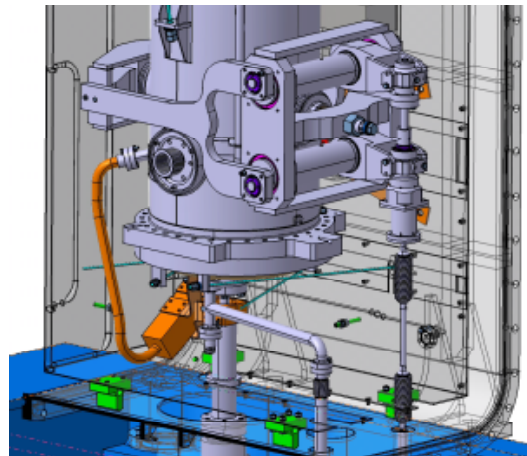


Figure 3: Layout of the CTS

#### 3.3 Helium pressure effects

The liquid helium distribution is expected to maintain pressure fluctuations inside the He tank within 1 mbar. The induced resonant frequency variations should be kept small enough, typically a tenth of cavity bandwidth, otherwise they would rapidly become a burden for the RF system. The frequency sensitivity  $|df/dP|$  has to be smaller than 13 Hz/mbar since the cavity bandwidth is 130 Hz. The main contribution to the detuning results from the deformation of the half torus shape at the top of the cavity which

leads to the vertical displacement of the stem. The adjustment of the Nb thickness to 4 mm on the whole cavity ensures a sensitivity of -2.5 Hz/mbar, which is a safe value. An optional stiffener has been studied in order to reduce  $df/dP$  to -1 Hz/mbar if necessary.

### 3.4 $\beta=0.07$ prototype cavity

The prototype differs from the final cavity since its construction was launched much earlier in the project, and the main objectives were to demonstrate the operation at high peak fields and thus validate the RF design, and develop fabrication procedures. The major differences are the 3 mm wall thickness instead of 4 mm, the NbTi removable bottom plate and NbTi flange compatible with Helicoflex gaskets. The prototype was manufactured from RRR>200 Niobium. The torus was formed by deep drawing. The stem was rolled from a sheet on a conical dye and electron-beam welded with a single weld. The drift tubes were CNC machined from a rod.

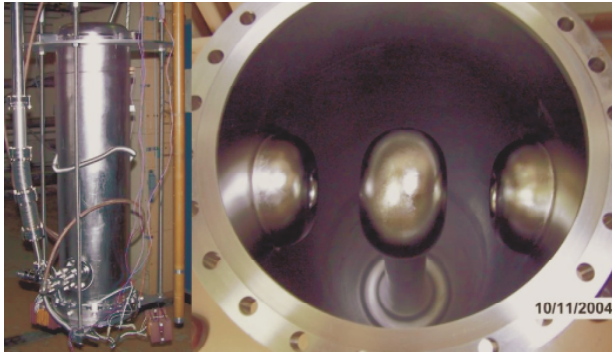


Figure 4:  $\beta=0.07$  prototype cavity

A custom HPR system with 9 nozzles has been designed and installed in the clean room. A standard 1-1-2 FNP chemical polishing was applied to the cavity in a closed loop. The resonator was then rinsed for 3 hours at 60 bars. During HPR, the cavity is slowly translated and rotated at the same time while the nozzle system remains still.

### 3.5 Tests in vertical cryostat

For this tests, instead of using an Helicoflex gasket, a special copper ring and indium seal was installed in the flange groove. During the first test, the cavity could reach an accelerating field of 9.5 MV/m for a  $Q_0$  of  $8 \cdot 10^8$  well above the SPIRAL 2 requirements (fig. 5).

Above this value, it becomes thermally unstable and the  $Q_0$  drops by 50 %, reaching a new equilibrium state. The cavity was equipped with thermal sensors in order to investigate on this instability. A second measurement showed that the stem and the torus region were not affected by this instability, but all the sensors located on the bottom flange and bottom plate showed a temperature increase. The He bath was pumped to reach 1.7 K in order to check if a better cooling of the copper ring would move the instability

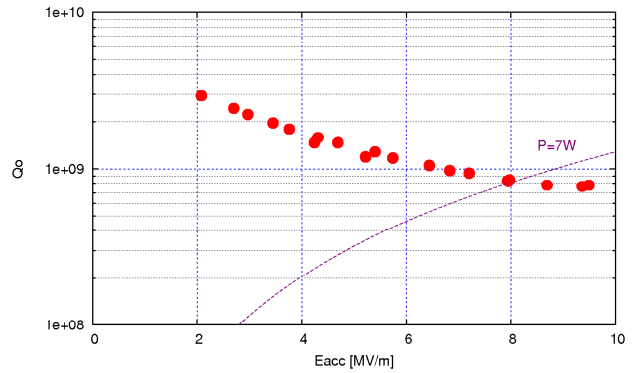


Figure 5:  $\beta=0.07$  prototype cavity 4 K test

threshold, but it was displaced to 10 MV/m. The cavity was then opened to replace the copper ring by a Nb sputtered and thicker copper ring to eliminate any normal conducting material on the RF surface. The cavity behavior did not change from the previous tests, a clear indication that the faulty part is the NbTi plate where a partial quench could occur. Given the magnetic field distribution in the lower part of the cavity and the extra power dissipated by the quenched part, we can estimate the area of the quenched RF surface and the corresponding power density. Thermal simulations of the NbTi plate using these parameters were carried out to check the consistency of this hypothesis. They show that due to the very low thermal conductivity of NbTi (0.3 W/m.K) combined with the thickness of the plate which prevents He bath from cooling it efficiently, the equilibrium state is a localized quench, unable to propagate to the whole plate. Since the bottom plate design of the final cavity is completely different, this issue is irrelevant for the linac.

During 4 K to 1.7 K pumping the resonant frequency of the cavity was recorded. The pressure sensitivity of -11 Hz/mbar was derived from this measurement. It differs from the value of -4.3 Hz/mbar that was computed for a cavity with a uniform thickness of 3 mm. The thickness was then measured with an ultrasonic probe, and a thickness reduction to 2 mm was discovered on the torus. This could be explained by the combination of the deep drawing process and a possibly nonuniform chemical polishing, since the fresh acid was injected in the torus region with the cavity sitting on its top. A new computation was carried out taking this parameter into account leading to a new  $df/dP = -11.1$  Hz/mbar, which is very close to the measured value. This emphasizes the strong influence of the torus thickness on the frequency stability. The measured Lorentz detuning coefficient is  $-1.7$  Hz/(MV/m)<sup>2</sup>.

## 4 $\beta=0.12$ RESONATORS

### 4.1 Mechanical design

The high  $\beta$  QWR was studied by IPN Orsay [9]. In contrast with the lower  $\beta$  QWR the high  $\beta$  resonators bottom part

is a welded Nb cap. Since the cavity can not be opened for rinsing, two ports are provided on the bottom cap to insert the HPR pipe, and two such ports are present at the top of the cavity rotated 90 degrees from the top pair to extend the rinsed area. The stainless steel He tank is attached to the cavity close to the bottom cap using a stainless steel ring brazed to the Nb outer cylinder.

#### 4.2 He pressure effect

The cavity wall thickness is 4 mm in order to withstand the He pressure bursts. The stem thickness can be safely reduced to 3 mm. A conical stiffener is welded on the top torus to reduce the vertical displacement of the stem when external pressure is applied (fig. 6).

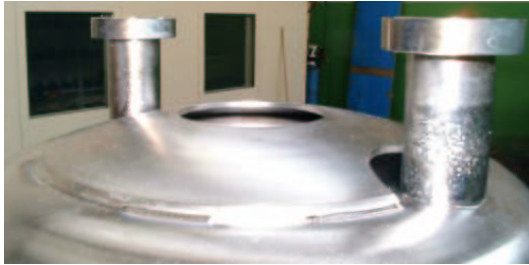


Figure 6:  $\beta=0.12$  torus stiffener

The structural calculations have been carried out using COSMOS, which can be coupled to the MICAV RF solver to compute frequency shifts resulting from deformations. The computed pressure sensitivity is  $-4.5$  Hz/mbar ( $-5.5$  Hz/mbar without stiffener). Since the  $\beta=0.12$  QWR bandwidth is 80 Hz, the expected frequency excursions due to 1 mbar pressure fluctuations is less than  $1/10^{th}$  of the bandwidth.

#### 4.3 Cavity Tuning

The tuning is split into static and variable tuning. The variable tuning system is still under study and could be performed using a cold tuning system similar to the Saclay tuner (fig. 7-a) or a movable superconducting plunger located inside one of the HPR ports (fig 7-b).

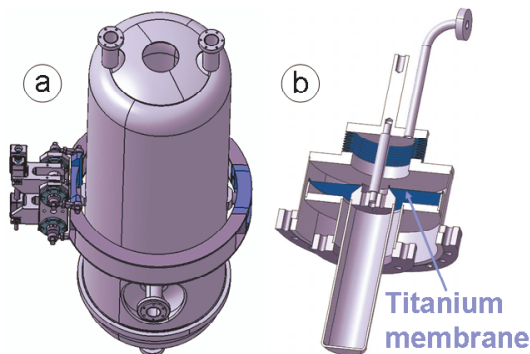


Figure 7:  $\beta=0.12$  tuners

By deforming the cavity (tuner a), due to the geometry and the surface field distribution of the  $\beta=0.12$  cavity, the tuning efficiency is reduced to  $\pm 4$  kHz/mm, giving a total tuning range of  $\pm 8$  kHz. Using the movable SC plunger (tuner b), the tuning range should be around  $\pm 2$  kHz.

Therefore an initial frequency correction may be necessary to ensure that the 4 K goal frequency is inside tuning range. This is achieved using one superconducting static plunger located inside one of the HPR ports on top of the cavity. By choosing the right diameter (from 15 to 30 mm max) and the right length of the plunger, we can shift the cavity frequency up to  $+70$  kHz.

#### 4.4 $\beta=0.12$ prototype cavity

The prototype cavity was built using the same Nb than the low  $\beta$  QWR. A frequency adjustment was performed before the welding of the external drift tubes by sliding them to their final position (fig. 8).



Figure 8:  $\beta=0.12$  QWR during frequency adjustment

Although the He tank was not needed for the 4K tests, the stainless steel ring was brazed to the cavity external cylinder to prove the feasibility of this large diameter joint. The chemical polishing, high pressure rinsing and clean room preparation were carried out at Saclay. The HPR equipment was specifically designed for the high  $\beta$  resonator. The 6 openings in the cavity were used in turn with a single stem-nozzle system.

#### 4.5 Tests at 4 K

The cavity was then tested at IPN-Orsay in a modified vertical cryostat. During 4 K RF test, the cavity exceeded the required performance, since the maximum accelerating field was 11 MV/m for  $Q_0=10^9$ , limited by the RF amplifier, with a low field  $Q_0$  of  $10^{10}$  (red curve fig. 9). The dissipated power at 6.5 MV/m was 4W (below the required

limit of 10W). A strong multipacting barrier was observed at very low field, i. e.  $E_{acc} < 50$  kV/m. Several hours were needed to go through it but it could not be conditioned. Another MP barrier was observed near 1.5 MV/m but it was passed easily within a few minutes. After leaving the cavity between 80 K and 120 K during 5 days, the 100K effect was observed (orange curve).

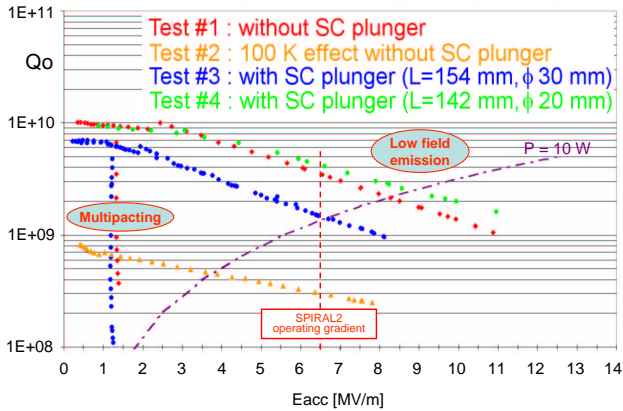


Figure 9:  $\beta=0.12$  prototype cavity 4 K tests

After that, two different SC plungers were tested on the cavity (blue and green curves). The biggest plunger detuned the cavity by +65 kHz and led to very promising result since the low field  $Q_0$  was only reduced by 30 %, and a quench occurred at 8 MV/m. A more recent test was carried out with a thinner plunger (20 mm diameter instead of 30 mm) and consequently more efficiently cooled for which the  $E_{acc}$  of 11 MV/m was reached without quench. The measured Lorentz detuning coefficient during these tests was  $-1.58$  Hz/(MV/m)<sup>2</sup>.

## 5 CRYOSTATS

Both low and high  $\beta$  cryostats (fig. 10) use a copper thermal shield cooled by He gas to 60 K. The evaluated static losses at 4 K for the low  $\beta$  module are 3 W and less than 10 W for the high  $\beta$  module, and respectively 25 W and 65 W at 60 K. They have to be partly assembled in a clean room together with the QWRs, power couplers, beam tubes, upstream and downstream vacuum gate valves. The cavities are supported by two sets of tension rods: antagonists rods for horizontal positioning and a set of vertical rods attached to the top of the cryostat which should bear the weight of the cavity.

## 6 CONCLUSION

Both QWR prototypes have been tested in a vertical cryostat and have exceeded the requirements on their electromagnetic properties. At the nominal accelerating field the dissipated power is 4 W for both  $\beta=0.07$  and  $\beta=0.12$  QWRs. The next step is to build two cryostats, one for each  $\beta$ , and equip them with cavities in order to test the resonators in operating conditions.

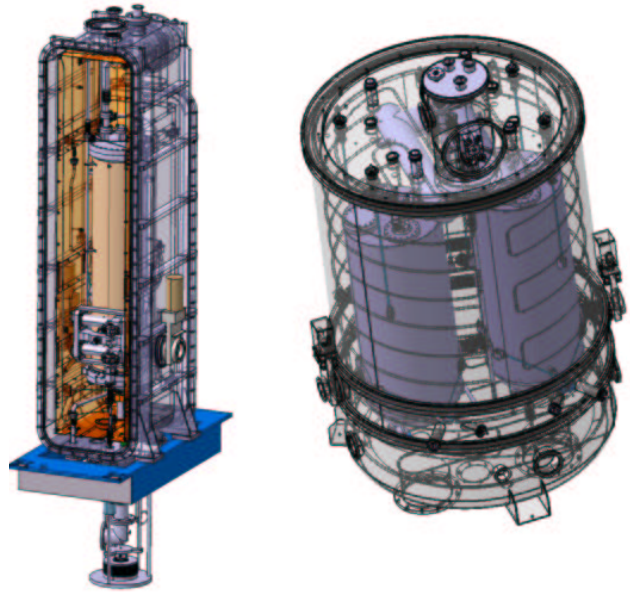


Figure 10: low (left) and high (right)  $\beta$  modules

## 7 ACKNOWLEDGEMENTS

The author wishes to thank G. Olry for providing informations on  $\beta=0.12$  cavity and Orsay and Saclay teams which participated to the SPIRAL 2 cavities development and tests.

## 8 REFERENCES

- [1] A. Mosnier et al., The design of the high intensity exotic beams SPIRAL 2 project, PAC 2005, Oak Ridge, May 2005.
- [2] A. Facco et al., Status of the Non-RFQ Resonators of the PIAVE Heavy Ion Linac, EPAC 2000, Vienna, May 2000.
- [3] K. W. Shepard, Status of Low and Intermediate Velocity Superconducting Accelerating Structures PAC 2003, Portland, May 2003.
- [4] R. Laxdall, Recent progress in the superconducting RF program at TRIUMF/ISAC, these proceedings
- [5] R. Duperrier et al., Status report on the beam dynamics developments for the SPIRAL 2 project, EPAC 2004, Luzern, June 2004.
- [6] T. Junquera et al., High intensity linac driver for the SPIRAL 2 project, EPAC 2004, Luzern, June 2004.
- [7] P. Bosland et al. Third harmonic superconducting passive cavities in ELETTRA and SLS, 11<sup>th</sup> SRF workshop, Travemünde, September 2003.
- [8] P. E. Bernaudin et al., Design of the low beta, quarter wave resonator and its cryomodule for the SPIRAL 2 project, EPAC 2004, Luzern, June 2004.
- [9] G. Olry et al., Development of beta 0.12 88 MHz quarter wave resonator and its cryomodule for the SPIRAL 2 project, these proceedings.